

A Multi-objective and Multi-level Optimization of IPMSM: Case Study Dynamometer

Ali Amini¹, MohammadSadegh KhajueeZadeh², Abolfazl Vahedi³

¹Iran University of Science and Technology/Department of Electrical Engineering, Tehran;
al_amini76@elec.iust.ac.ir

²Iran University of Science and Technology/Department of Electrical Engineering, Tehran;
mohammadkhajuee@yahoo.com

³Iran University of Science and Technology/Department of Electrical Engineering, Tehran;
avahedi@iust.ac.ir

Abstract

In dynamic-drive tests on electric motors, the dynamometer has a key role. An AC dynamometer has advantages such as higher dynamics, efficiency, and reliability among the other categories like eddy current brake. Since the accuracy of measurement in dynamic tests has a high dependency on the AC dynamometer's operating condition, proposing an electric motor with advantages including high efficiency, high safety factor, low vibration, and low noise is a big concern. Accordingly, a multi-objective (electrically and mechanically) and multi-level (geometry and drive) design is the aim of this study. An Interior Permanent Magnet Synchronous Motor (IPMSM) is the case study. Through surrogate modeling and Particle Swarm Optimization (PSO) algorithm (more time-efficient and accurate than classic algorithms), the final design is suggested. Finally, comparing the initial and final designs will show the fulfillment of all objectives, mechanically and electrically.

Keywords: Alternating Current (AC) Dynamometer, Interior Permanent Magnet Synchronous Motor (IPMSM), Multi-physics Optimization, Particle Swarm Optimization (PSO) algorithm, Surrogate Model, Multi-level Optimization.

Introduction

A necessary stage after designing an electric motor is a dynamic-drive test (Besides the static-drive test) through dynamometer systems. The above tests give a vision of operating conditions, leading to higher-quality manufacturing. On the contrary, a lack of dynamic tests might lead to severe damage. Dynamometer contains an electric machine or a brake structure, while its axis has a coupling connection with the under-test motor as a load, as shown in Figure. 1 (Different operating regime). Due to the complexity of industry loads, break-structure dynamometers, such as eddy current brakes, cannot give satisfactory accuracy, thermal stability, low inertia, and reliability [1]. Accordingly, AC dynamometers (with an electric machine) are paying attention. The used electric machine in AC dynamometers is usually categorized into two groups: Induction Machines (IMs) and Permanent Magnet Machines (PMMs), which act in motor or generator operating modes.

One of the highlight merits of AC dynamometer over brake structures is negligible energy loss [2]. In brake structure, a mighty energy loss is through heat, whereas energy wasting is significantly lower in AC dynamometer

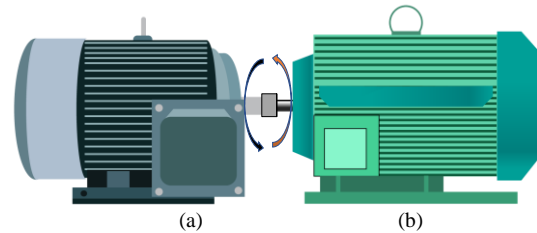


Figure 1. Schematic of test bench with employing AC dynamometer: (a) motor under test (b) load machine.

systems owing to energy reversing to the grid (using inverters). Based on the advantages of an AC dynamometer, the electric motor must have, on the one hand, low inertia, low *Torque Ripple* (T_{ripple}) and *Cogging Torque* ($T_{cogging}$), high efficiency, and high *Maximum Torque* (T_{max}). On the other, it is a measurement tool which low lateral vibration, low noise, high stiffness, and high safety factor that are a necessity. The IMs have low dynamic and complexity in the control algorithm, leading to more attention to PMMs [3]. PMSMs are categorized based on how implementing Permanent Magnets (PMs) into Interior PM (IPM) and Surface PM (SPM). As shown in Figure. 2, the first has the benefit of *Reluctance Torque* ($T_{reluctance}$) along with *Electromagnetic Torque* ($T_{electromagnetic}$), leading to higher T_{max} . On the other hand, SPM has lower T_{ripple} . Moreover, IPM has no thin fiber to restrain centrifugal force [4]. So, in this study, IPM is the regarded geometry.

According to the diversity in electric motor usage, the possibility of proposing a generalized geometry to meet all constraints and objectives is near zero. i.e., in an AC dynamometer, both objectives, electrically and mechanically, must be regarded, which initial designs cannot give them simultaneously. This fact is a testimony for requiring optimization. Although numerous designs were suggested optimally on IPMs [5], [6], each has a deficiency, such as neglecting the effect of the rotor or stator, not considering the mechanical objectives, and not

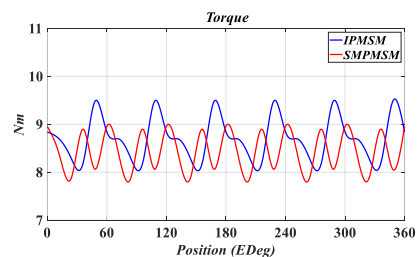


Figure 2. Comparing the *Torque* between IPMSM and SMPMSM.

investigating the effect of drive level. Besides all the above, proposing a geometry with the lowest design time and highest accuracy is a big honor, which surrogate modeling gives (contrary to classic algorithms).

In the following study, after introducing the regarded IPM as the case study, the methodology of the suggested multi-objective multi-level design will be given comprehensively. Finally, comparing the initial and final designs will show the fulfillment of all objectives, mechanically and electrically.

Case Study

By taking advantage of design guidelines in [7], the initial design will be yielded. It must be highlighted that this electric motor is for use in AC dynamometers, so considering some of the constraints, even in the initial design, is mandatory. i.e., a higher ratio of motor length to Pole Pitch in order to have lower inertia. Moreover, the employed winding configuration is Distributed. So, owing to its mitigation effect on coil Pitch, the short type will be regarded, where the short Pitch coil will mitigate high-order stator harmonics [8]. The technical data of the initial design is given in Table 1. The topology of the initial design is displayed in Figure. 3.

Multi-objective and Multi-level Optimization

In this study, through surrogate modeling besides Particle Swarm Optimization (PSO) algorithm, our multi-objective and multi-level (geometry and drive levels) design will be yielded. Accordingly, six objectives are regarded to reach the best geometry, mechanically and electrically, including T_{ripple} , T_{max} , efficiency, safety factor, Average and Maximum of lateral vibration (Displacement). In Figure. 4, the methodology of multi-level multi-objective optimization is shown. Details of each level and its objectives are as below:

A. Geometry Level

In the beginning, the geometry level and its objectives will be investigated comprehensively to get the best design in the rotor and stator geometrically.

Table 1
Technical design data of the initial design

Designed Parameters	Unit	Value
Number of Phases	-	3
Number of Poles	-	8
Phase Advance	Elec Deg	45
Air Gap	mm	0.55
Coil Pitch		5
Copper Slot Fill Factor		0.41
Hard Magnet	-	N42SH
Soft Magnet		M250-35A

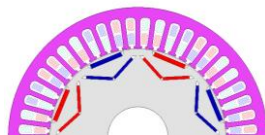


Figure 3. Topology of the designed IPMSM.

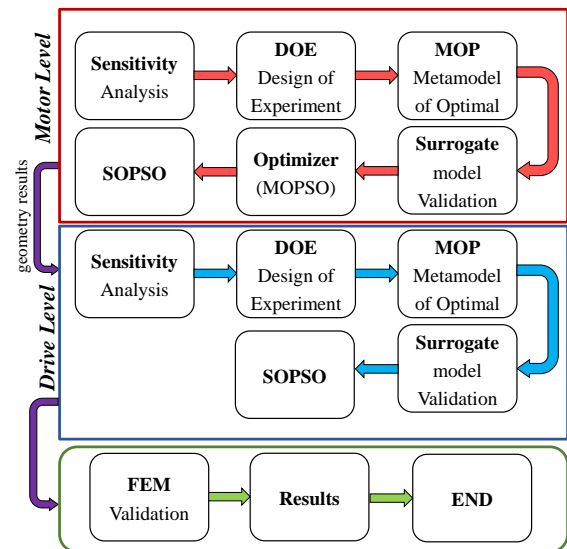


Figure 4. The methodology of multi-level multi-objective optimization.

A.1. Sensitivity Analysis

It is mandatory that using sensitivity analysis (as displayed in Figure. 5) to recognize the most effective design variables (in Figure. 6 and Table 2) on motor operating conditions. One of the great challenges in motor design is geometry errors, which using variables in ratio format can overcome it appropriately. i.e., slot ratio.

A.2. Surrogate Model and Design of Experiment (DOE)

According to numerous designs and objectives, Time-stepping Finite Element Analysis (TSFEA) will be significantly time-consuming. So, using surrogate modeling can facilitate this aim. Since the accuracy of surrogate modeling has a high dependency on the number of designs, the Latin Hypercubes (LHS) is the chosen sampling methodology owing to its merits, as written in [9]. After providing a satisfactory DOE (about 1700 designs), training the six accurate Surrogate Models (SMs) as the connection between geometry and objective is the next stage. The Anisotropic Kriging (advantageous in local non-linear modeling) is the employed algorithm for surrogate modeling, where the train and test data sets are %80 and %20 of DOE, respectively.

It is necessary that the accuracy of SMs must be investigated, which Mean Normalized Error (MNE) and R^2 score are as its metrics. Whatever the MNE is closer to zero and R^2 is almost near to one, the accuracy is higher. In Table 3, assessment of the SMs is shown. Higher accuracy brings the expectancy of more similarity between the algorithm results and TSFEA.

A.3. PSO Algorithm

The final stage is the PSO algorithm [10], which has advantages such as the ability to global search and high-accurate designs. Its how-working flowchart is displayed in Figure. 7. The termination criterion in this study is the number of generations (10000). Between 10000 designs, 219 designs don't meet the objective constraints (Unfeasible). Additionally, 1226 designs were recognized as Pareto front. In order to find the best design, a metric

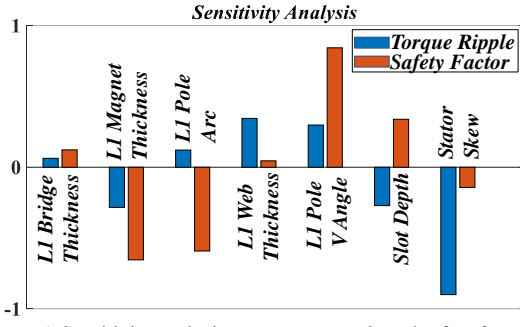


Figure 5. Sensitivity analysis on T_{ripple} and safety factor.

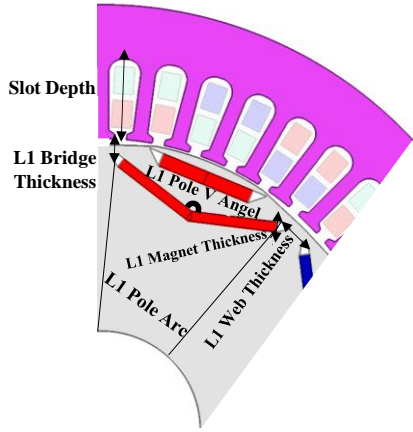


Figure 6. Geometry guide for design variables.

Table 2
Variables of the geometry-level optimization

Optimization Variables	Unit	Min	Max
L1 Bridge Thickness	mm	2.5	8.0
L1 Magnet Thickness	mm	1.0	3
L1 Pole V Angle	MDeg	95	150
Stator Skew	MDeg	2.5	7.25
L1 Web Thickness	Ratio	0.1	0.9
L1 Pole Arc	Ratio	0.7	0.9
Slot Depth	Ratio	0.66*	0.8

* Considering the maximum slot fill factor of about %50.

must be written (F_{min}) which considers the objectives simultaneously, according to the weighting coefficients of each, as shown in (1). Choosing the weighting coefficients has a dependency on effectiveness, where safety factor and T_{ripple} are our nominators for the highest coefficients. According to F_{min} (in Figure. 8), the ID design of 5491 is the best geometry, where the status of the geometry variables in this design is shown in Table 4.

B. Drive Level

Besides the motor geometry, drive control has a significant role in T_{ripple} , which shows the necessity of multi-level designs (drive level after geometry level). This

Table 3
Accuracy assessment of the trained Surrogate Models

Objective and Constraint	MNE	R^2
Maximum torque	0.004	1
System efficiency	0.005	9.99e-1
Torque ripple	0.041	9.61e-1
Rotor Lamination displacement average	0.003	1
Rotor Lamination displacement max	0.001	1
Safety factor	0.044	9.31e-1

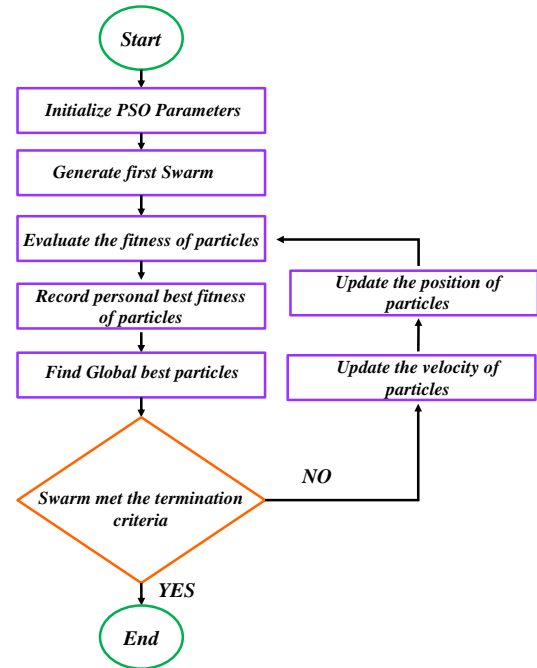


Figure 7. Flowchart of the PSO algorithm.

study tries to reach a smoother T_{ripple} through changing the Phase Advance in the drive system (as shown in Figure. 9). The sensitivity analysis endorses the effect of Phase Advance only on T_{ripple} not the other objectives. Procedure of optimizing drive level is analogous to geometry level.

C. Verifying with FEA

It is mandatory that the suggested design in view of geometry and Phase Advance (33.13°) be verified through TSFEA. In Table 5, the good agreement between PSO results and TSFEA is shown.

Performance Assessment

After verifying the final design through TSFEA, assessment its operating conditions, electrically and mechanically, is the end task as an engineer.

$$F_{min} = c_1 \times \frac{\text{Initial Maximum Torque}}{\text{Maximum Torque}} + c_2 \times \frac{\text{Rotor Lamination Displacement Average}}{\text{Initial Rotor Lamination Displacement Average}} + c_3 \times \frac{\text{Rotor Lamination Displacement Max}}{\text{Initial Rotor Lamination Displacement Max}} + c_4 \times \frac{\text{Initial Safety Factor}}{\text{Safety Factor}} + c_5 \times \frac{\text{Initial Efficiency}}{\text{Efficiency}} + c_6 \times \frac{\text{Torque Ripple}}{\text{Initial Torque Ripple}} \quad (1)$$

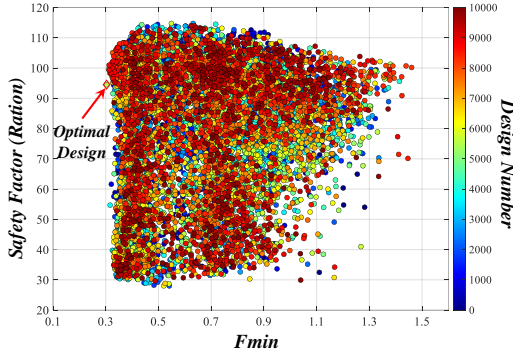


Figure 8. Fmin in generations of PSO algorithm (for brevity, it is shown just for safety factor).

Table 4
Design variables after the geometry-level optimization

Optimization Variables	Unit	Value
L1 Bridge Thickness	mm	2.9013
L1 Magnet Thickness	mm	2.2819
L1 Pole V Angle	MDeg	149.3737
Stator Skew	MDeg	7.25
L1 Web Thickness	Ratio	0.461
L1 Pole Arc	Ratio	0.8268
Slot Depth	Ratio	0.66

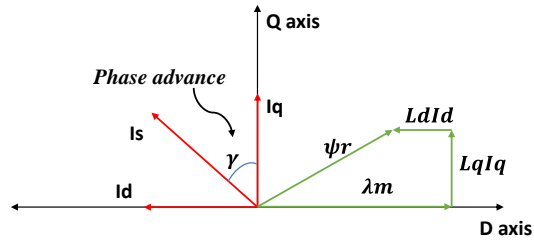


Figure 9. Concept of Phase Advance in the d - q reference frame.

Table 5
Comparing the PSO results and TSFEM (verifying)

Optimization Objective	Unit	Value	
		Algorithm	FEM
Maximum torque	Nm	122.5	122.6
System efficiency	%	96.2	96.2
Torque ripple	%	6.1	6.2
Rotor Lamination displacement Average	mm	0.0003	0.0003
Rotor Lamination displacement Maximum	mm	0.0004	0.0004
Safety factor	Ratio	94.5	94

A. Electrical Characteristics

Comparing the electrical characteristics between the initial and final geometry shows that tangential flux density of air-gap has become sinusoidally, and its maximum has become lower. Moreover, improving T_{ripple} and $T_{cogging}$, %80 and %91, respectively, are the other significant effect of the suggested geometry.

Reducing the T_{max} is negligible. In Figure. 10, T_{ripple} , $T_{cogging}$, and tangential flux density of air-gap are shown, which are the most effective electrical characteristics in the dynamometer. Additionally, efficiency is higher than %95, which is satisfactory.

B. Mechanical Characteristics

Mechanical analysis is one of the most necessary investigations in the electric motors field, especially the AC dynamometer (which has a significant effect on dynamic drive tests). Accordingly, our analysis shows that the suggested geometry has lower mass, T_{ripple} , and consequently lower stress (analysis on the rotor as the load carrier). On the other hand, according to the yield stress similarity in both geometry (initial and final designs), the suggested design gives a higher safety factor.

Since the force on the rotor body has a dependency on angular velocity and mass ($m\omega^2 e \cos \omega t$) [11], improving T_{ripple} and lower mass leads to lower force. So, based on the stiffness, lower force in the same material brings lower lateral vibration and noise [12], as shown in Table 6 and Figure. 11. Besides lateral vibration, the lateral natural frequency is the other significant subject, effective in operating conditions and angular velocity. Accordingly, the redline of the initial design is in 5500 rpm, 7800 rpm, and 9800 rpm, which in the final design is only in 8800 rpm.

Conclusion

In this study, proposing an IPM to use in AC dynamometers was regarded, which meets the constraints, mechanically and electrically. Based on the best knowledge of authors, previously, IPM was not designed

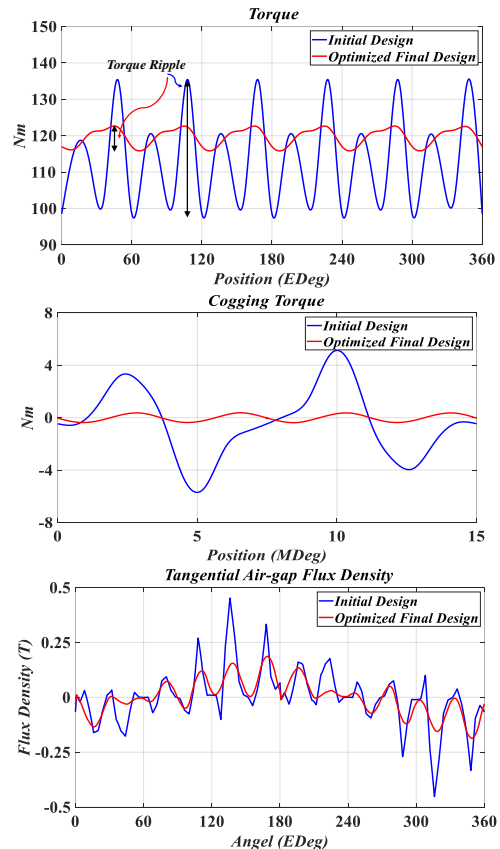


Figure 10. Comparing the initial and final designs.

Table 6
Comparing the mechanical objectives between the initial and final designs

Optimization Objective	Unit	Value	
		Optimized Final Design	Initial Design
Rotor Lamination Displacement Average	mm	0.0003	0.0007
Rotor Lamination Displacement Maximum	mm	0.0004	0.002
Rotor Lamination Stress Maximum	MPa	4.9	28.1
Safety Factor	Ratio	93.97	16.38

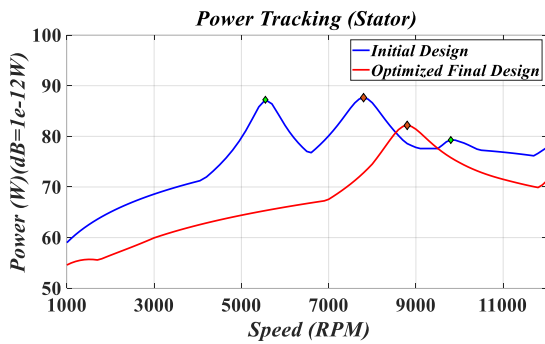


Figure 11. Comparing acoustic curves in both initial and final designs.

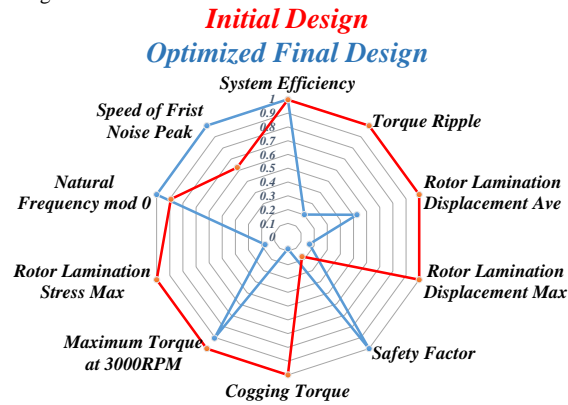


Figure 12. A summary of comparing both the initial and final designs (before and after multi-objective and multi-level optimization).

to use in dynamometer. Accordingly, the redesign objectives are low T_{ripple} , low $T_{cogging}$, low inertia, low lateral vibrations, low noise, high efficiency, and high safety factor. A delta-type IPM was the case study. Through surrogate modeling (time-efficient and accurate according to MNE and R^2 metrics) along with the PSO algorithm, the final design was suggested, which has merits (as displayed in Figure. 12) such as lower T_{ripple} (%79.75), low $T_{cogging}$ (%95), lower lateral vibrations (%47.43 in average and %83.55 in maximum), and higher safety factor (%473.68). Moreover, increasing the angular velocity and decreasing the noise level in the first crest are significant.

References

- [1] J. Arellano-Padilla, G. M. Asher, and M. Sumner, "Control of an AC Dynamometer for Dynamic Emulation of Mechanical Loads With Stiff and Flexible Shafts," *IEEE Transactions on Industrial Electronics*, vol. 53, no. 4, pp. 1250–1260, Jun. 2006, doi: 10.1109/TIE.2006.878309.
- [2] "www.dynamometers.org."
- [3] A. Tahir *et al.*, "Evaluating the value of the excitation capacitance of a wind turbine/induction generator system using genetic algorithms," in *2017 8th International Renewable Energy Congress (IREC)*, Mar. 2017, pp. 1–6. doi: 10.1109/IREC.2017.7926045.
- [4] H. Xu, H. Geng, H. Lin, Y. Qi, and X. Yin, "Rotor Design and Analysis of a High Speed Permanent Magnet Synchronous Motor for Cryogenic Centrifugal pump," in *2019 IEEE International Conference on Mechatronics and Automation (ICMA)*, Aug. 2019, pp. 1756–1760. doi: 10.1109/ICMA.2019.8816583.
- [5] S. Ahmadi, T. Lubin, A. Vahedi, and N. Taghavi, "Sensitivity-based optimization of interior permanent magnet synchronous motor for torque characteristic enhancement," *Energies (Basel)*, vol. 14, no. 8, 2021, doi: 10.3390/en14082240.
- [6] J. Soleimani, A. Vahedi, and S. M. Mirimani, "Inner permanent magnet synchronous machine optimization for HEV traction drive application in order to achieve maximum torque per ampere," *Iran. J. Electr. Electron. Eng.*, vol. 7, pp. 241–247, 2011.
- [7] Hamdi and Essam S, *Design of small electrical machines*, Four. 1995.
- [8] R. Deshmukh, A. J. Moses, and F. Anayi, "Voltage harmonic variation in three-phase induction motors with different coil pitches," *J Magn Magn Mater*, vol. 304, no. 2, pp. e810–e812, Sep. 2006, doi: 10.1016/j.jmmm.2006.03.005.
- [9] F. Farshbaf Roomi, A. Vahedi, and S. A. Mirnikjoo, "Multi-Objective Optimization of Permanent Magnet Synchronous Motor Based on Sensitivity Analysis and Latin Hypercube Sampling assisted NSGAI," in *2021 12th Power Electronics, Drive Systems, and Technologies Conference, PEDSTC 2021*, 2021. doi: 10.1109/PEDSTC52094.2021.9405918.
- [10] S. Fang, Y. Wang, W. Wang, Y. Chen, and Y. Chen, "Design of Permanent Magnet Synchronous Motor Servo System Based on Improved Particle Swarm Optimization," *IEEE Trans Power Electron*, vol. 37, no. 5, pp. 5833–5846, May 2022, doi: 10.1109/TPEL.2021.3128188.
- [11] M. S. Khajuee Zadeh, Z. Nasiri-Gheidari, and F. Tootoonchian, "Study of Noise and Vibration in Wound Rotor Resolvers," in *2020 28th Iranian Conference on Electrical Engineering (ICEE)*, Aug. 2020, pp. 1–5. doi: 10.1109/ICEE50131.2020.9260668.
- [12] M. S. Khajueezadeh, S. FeizHoseini, Z. Nasiri-Gheidari, and M. Behzad, "Analysis of Torsional

Vibrations on the Resolver Under Eccentricity in PMSM Drive System,” *IEEE Sens J*, vol. 22, no. 22, pp. 21592–21599, Nov. 2022, doi: 10.1109/JSEN.2022.3209991.